

Second-law energy efficiency as performance indicator for heat and energy recovery ventilators

Magnus Aa. Gjennestad^a, Eskil Aursand^b, Elisa Magnanelli^{c,*}, Jon Pharoah^d

^a*Department of Physics, NTNU - Norwegian University of Science and Technology
NO-7491 Trondheim, Norway*

^b*Department of Energy and Process Engineering,
NTNU - Norwegian University of Science and Technology
NO-7491 Trondheim, Norway*

^c*Department of Chemistry, NTNU - Norwegian University of Science and Technology
NO-7491 Trondheim, Norway*

^d*Department of Mechanical and Materials Engineering, Queen's University
K7L 3N6 Kingston, Canada*

Abstract

The increasing attention to energy savings has contributed to the increased use of energy recovery systems for building ventilation. However, the use of such systems might not be always beneficial from an energy point of view. We investigate the efficiency of these systems under different outdoor conditions using second-law analysis. This analysis makes it possible to assess performance in terms of loss of work potential, and to account for the different quality of energy. We use the second-law energy efficiency as single performance parameter, in contrast to the several indicators commonly used to characterize recovery systems. We consider and compare the performance of a heat recovery ventilator (HRV) with that of a structurally similar membrane energy recovery ventilator (MERV) which can exchange both heat and moisture.

We show that the second-law efficiency can be used to identify the range of operating conditions for which the recovery ventilator is not beneficial as the energy cost is greater than the energy recovery. This is not trivial using traditional performance parameters, yet it is a natural outcome of the second law analysis. In addition we identify the location and the mechanism by which work potential is lost, which can help the eventual optimization of both the recovery process and the devices used to carry them out.

Keywords: second-law efficiency, energy efficiency, recovery ventilator, ventilation systems

*Corresponding author. Tel.: +47-73594183

Email address: elisa.magnanelli@ntnu.no (Elisa Magnanelli)

1. Introduction

The increased attention to energy savings has led to buildings becoming more heavily insulated [1, 2]. However, in buildings with tight envelopes, air quality becomes an issue as pollutants may rapidly build up to dangerous levels [3–5]. In order to ensure good air quality, it is increasingly important to install ventilation systems that exchange indoor air with fresh outdoor air [6, 7].

Temperature and humidity are parameters that play a vital role in the indoor environment and they should be maintained within certain limits to ensure comfort and health [8]. This can be a challenge in both cold climates, where outdoor air coming in through the ventilation system can be much colder and drier than is optimal, and in warm climates where the outdoor air may be too moist and warm. Auxiliary heating, air-conditioning, humidification and dehumidification systems are necessary to compensate for differences between the conditions of the incoming air and the desired indoor conditions.

In recent years, an increased demand for indoor comfort, together with an increase in time spent indoors has increased the energy use of buildings to the same level as that of the transport and industry sectors [9–11]. This has resulted in the installation of heat recovery systems, which are nowadays often required by regulations and codes in order to reduce building energy consumption [12–14].

Heat and energy recovery ventilators (HRV/ERV) are devices that transfer heat, or both heat and moisture, from one air stream and deliver it to another [15]. Numerous types of recovery ventilators are currently available, having different characteristics and performance [16].

A widespread solution for heat recovery is the flat plate heat exchanger, which is often used due to low capital costs and ease of operation [16]. In this device, the exhaust and fresh air streams exchange heat across the wall that separates them. In order to obtain large heat exchange surfaces, many parallel channels are usually stacked on top of each other [17]. A major limitation of this technology is that moisture cannot be transferred between the two air streams. For this reason, Zhang and Jiang [18] proposed an alternative solution to conventional flat plate heat exchangers that makes use of a water-permeable membrane as separating wall between the two air streams. In this way, the exhaust and the fresh air can exchange moisture in addition to heat.

The performance of a HRV/ERV is influenced by several factors, one of which is the ability to transfer heat from one air stream to the other. As long as the air moisture stays in vapor phase, only sensible heat is exchanged between the streams. However, if the cooled stream reaches the saturation temperature then water condenses [19] and the latent heat of condensation is released and is available to be transferred to the heated stream. Another factor is moisture recovery, which can be achieved in membrane-based energy recovery ventilators (MERV). A third factor is the additional fan power required to drive the air flow through the recovery system. While recovering energy from the exhausted air stream, HRVs/ERVs increase the electrical energy required by ventilation fans [20] and thus a net energy saving is not guaranteed.

Many works can be found in literature that assess the performance of recovery ventilators [18, 21–29]. Three performance indicators are traditionally considered. The first parameter, ϵ_s , accounts for the recovery of sensible heat and it is often defined

as [30]

$$\epsilon_s = \frac{T_{in}^{ex} - T_{out}^{ex}}{T_{in}^{ex} - T_0}, \quad (1)$$

where T_{in}^{ex} and T_{out}^{ex} are the temperatures of the exhaust air at the inlet and outlet of the recovery ventilator, respectively, and T_0 is the temperature of the outdoor ambient.

If water is condensed on the wall separating the air streams, latent heat is released, and a second performance parameter can be defined as [26]

$$\epsilon_h = \frac{H_{in}^{ex} - H_{out}^{ex}}{H_{in}^{ex} - H_0}, \quad (2)$$

where H_{in}^{ex} and H_{out}^{ex} are enthalpy flows entering and leaving the system with the exhaust air stream, and H_0 is the enthalpy flow that enters the ventilator with the fresh air stream.

In systems where water is also exchanged, a third performance indicator is used to describe the recovery of moisture [30]

$$\epsilon_w = \frac{x_{w,in}^{ex} - x_{w,out}^{ex}}{x_{w,in}^{ex} - x_{w,0}}, \quad (3)$$

where $x_{w,in}^{ex}$ and $x_{w,out}^{ex}$ are the water molar fractions of the exhaust air at the system inlet and outlet, and $x_{w,0}$ is the water molar fractions in the outdoor air.

While useful by themselves, these indicators are difficult to compare and relate to each other. Since there is no obvious optimal trade-off between them it is challenging to develop a global performance indicator that allows for a sensible comparison of different technical solutions and different types of recovery devices. Moreover, these parameters do not take into consideration the additional need for fan power. Indeed, a fundamental challenge with recovery ventilators is that they involve various energy forms (i.e. thermal energy, chemical potential energy, and electric energy), which differ from each other both from a thermodynamic and an economic point of view (e.g. a certain amount of heat at 294 K has less energy quality and it is in principle cheaper to produce than the same amount of electricity).

In this work, we investigate the efficiency of ventilation recovery systems using second-law analysis. This analysis makes it possible to assess the performance of HRV/ERV in terms of loss of work potential or, equivalently, in terms of entropy produced by the process [31]. The method allows for the definition of *one single parameter* to quantify the performance of the process, the second-law energy efficiency [32], which can account for the quality of different forms of energy. An easier and more meaningful comparison of different technical alternatives is therefore possible. In addition, it is possible to localise and quantitatively compare the different sources of lost work potential in the system, which may aid in design and optimization. This approach is in line with a part of the strategy of the American Society of Heating, Refrigerating and Air-Conditioning Engineers (ASHRAE), which has established a technical group named Exergy Analysis for Sustainable Buildings, to promote the use of concepts such as lost work for the assessment of energy use of buildings [33].

In our analysis, we include the losses due to pressure drops in the ventilation recovery system, and thus we account for the additional power consumed by fans. These

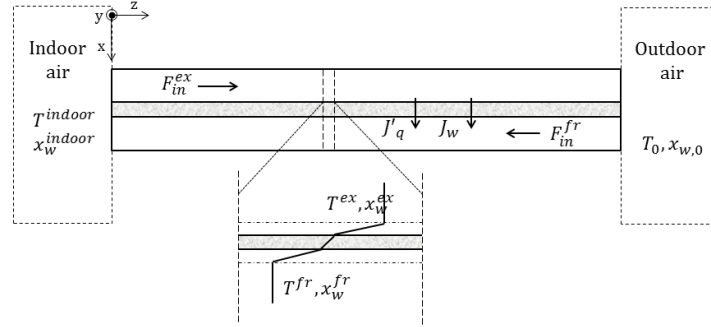


Figure 1: Schematic representation of the recovery ventilator. The exhaust air from the indoors flows parallel to the wall that separates the two sides of the system (z -direction). The fresh air from the outdoor ambient flows in opposite direction (counter-current configuration). Fluxes of heat, J'_q , and water, J_w , are exchanged across the separating wall (x -direction).

may contribute significantly to the overall losses [34] but they are often neglected in performance studies and are not reflected in the performance indicators that are used.

We will consider examples where we calculate and compare the second-law efficiency and the heat and moisture effectiveness of a flat plate HRV and those of a structurally similar MERV. We shall see how ambient conditions influence the second-law efficiency of the two systems in a non-trivial way, that cannot be predicted by the most commonly used heat and moisture effectiveness. We will consider ambient temperatures and relative humidities characteristic of both cold and warm climates.

After presenting the recovery systems in Section 2, the thermo-fluid dynamic model developed to describe the recovery ventilators is introduced in Section 3. In Section 4, we present the analyzed cases and the most relevant data. The solution procedure and model validation are illustrated in Section 5, before results are presented and discussed in Section 7. Conclusions are summarized in Section 8.

2. System

Figure 1 shows a schematic representation of a recovery ventilator. The exhaust air from the indoor environment flows from left to right in the positive z -direction, while the fresh stream from the outdoor ambient flows parallel to it, but in opposite direction. Since the two streams have different temperatures and composition, driving forces exist for heat and mass transport between them.

In the thermo-fluid dynamic description of the system, we make the following assumptions:

- the bulk of both gases is perfectly mixed in the x - and y -direction;
- temperature and concentration gradients in the x -direction are only present in the separating wall and in the convective boundary layers on both sides of it;
- diffusive fluxes along the z -direction are neglected, as they are small in comparison to the advective flow;

- the gas is considered to be an ideal mixture of ideal gases, where the only components are water and dry air;
- the dry air is assumed to be 79% molar fraction of nitrogen and 21% oxygen.

We consider and compare two structurally similar solutions for recovery ventilators. The two solutions have the same geometry, but differ in the structural and physical properties of the wall that separates the air streams:

Heat recovery ventilator (HRV): The wall separating the air streams is a metal plate. Therefore, only sensible heat can be transferred from one air stream to the other.

Membrane energy recovery ventilator (MERV): The wall separating the two streams is a water-permeable membrane. Both sensible heat and moisture can be exchanged between the two streams. We assume that water is the only component that can permeate the membrane.

The recovery performances of these systems depends greatly on the exchange surface between the two streams. Therefore, in practical applications, N pairs of exhaust/fresh air channels are stacked to obtain a suitable configuration for the system.

3. Theoretical formulation

In Section 3.1, we present the equations used to describe the spatial variation of the system thermodynamic variables. Section 3.2 deals with heat and mass transport across the system (x -direction). The description of transport makes use of the nonequilibrium thermodynamic framework [35]. In Section 3.3, we present the different contributions to the loss of work potential, and define the second-law energy efficiency for the system.

3.1. Balance equations

The thermodynamic driving forces between the two air streams cause transport of heat and mass from one side to the other. Humid air flows in the ducts, and the water mole fraction varies in space. Therefore, two mass balances are necessary to describe the system, one for the water content of air (subscript w) and one for the dry air (subscript a). At steady state, the mass balance equations for the exhaust air can be written as:

$$\frac{dF_w^{ex}}{dz} = -WJ_w \quad (4)$$

$$\frac{dF_a^{ex}}{dz} = -WJ_a = 0 \quad (5)$$

where F_w^{ex} and F_a^{ex} are the water and the dry air molar flow rates, W is the width of the duct (in the y -direction), and J_w and J_a are the molar fluxes across the wall separating the streams. Since the separating wall is impermeable to dry air, J_a equals zero and F_a^{ex} is constant. The total molar flow rate is given by the sum of the flow rates of the two components, $F^{ex} = F_w^{ex} + F_a^{ex}$.

Since we assume that the diffusive fluxes in the z -direction are negligible in comparison to the bulk flow velocity, the component flow rates can be related to the component mole fraction as:

$$F_i^{ex} = x_i^{ex} F^{ex} = x_i^{ex} c^{ex} v^{ex} A^{ex} \quad (6)$$

where x_i^{ex} is the mole fraction of the component i , c^{ex} is the total molar concentration of gas, v^{ex} is the molar velocity, and A^{ex} is the duct cross sectional area. We use the subscript i to indicate the different components, $i \in [w, a]$.

The pressure drop in a duct can be calculated by Darcy–Weisbach equation [36]:

$$\frac{dp^{ex}}{dz} = - \frac{v^{ex}}{|v^{ex}|} f^{ex} \frac{\rho^{ex} (v^{ex})^2}{2D_h^{ex}} \quad (7)$$

where f^{ex} is the friction factor, ρ^{ex} is the mass density, p^{ex} is the pressure, and $D_h^{ex} = \frac{4A^{ex}}{2W+2H}$ is the hydraulic diameter of the duct.

The energy balance of the exhaust air stream can be written as:

$$\frac{d(F^{ex} h^{ex})}{dz} = A^{ex} f^{ex} \frac{v^{ex}}{|v^{ex}|} \frac{\rho^{ex} (v^{ex})^3}{2D_h^{ex}} - W J_q \quad (8)$$

where h^{ex} is the molar enthalpy of the gas, and J_q is the total heat flux from the exhaust to the fresh air. The first term on the right-hand side of Eq. 8 represents the friction term. Applying the chain rule and substituting Eqs. 4 and 5 into Eq. 8, the energy balance can be rewritten in terms of the molar enthalpy as:

$$F^{ex} \frac{dh^{ex}}{dz} = A^{ex} f^{ex} \frac{v^{ex}}{|v^{ex}|} \frac{\rho^{ex} (v^{ex})^3}{2D_h^{ex}} - W (J_q - h^{ex} J) \quad (9)$$

where $J = J_w + J_a$ is the total molar flux through the separating wall. Equation 9 can be reformulated as an ordinary differential equation (ODE) for the temperature. For an ideal gas, the total enthalpy differential can be written as:

$$dh^{ex} = c_p^{ex} dT^{ex} + \sum_i h_i^{ex} dx_i^{ex} \quad (10)$$

where c_p^{ex} is the molar heat capacity, T^{ex} is the temperature, and h_i^{ex} is the partial molar enthalpy. Equation 9 can then be rewritten as:

$$c_p^{ex} \frac{dT^{ex}}{dz} = f^{ex} \frac{v^{ex}}{|v^{ex}|} \frac{M^{ex} (v^{ex})^2}{2D_h^{ex}} - \frac{W}{F^{ex}} (J_q - h^{ex} J) - \sum_i h_i^{ex} \frac{dx_i^{ex}}{dz} \quad (11)$$

where M^{ex} is the molar mass of the exhaust air.

All the thermodynamic variables introduced above refer to the exhaust air, and they are referred to with the superscript ex . We indicate the corresponding variables on the fresh air side with a similar notation and the superscript fr . The balance equations for

the fresh air are:

$$\frac{dF_w^{fr}}{dz} = WJ_w \quad (12)$$

$$\frac{dF_a^{fr}}{dz} = WJ_a = 0 \quad (13)$$

$$\frac{dp^{fr}}{dz} = -\frac{v^{fr}}{|v^{fr}|} f^{fr} \frac{\rho^{fr} (v^{fr})^2}{2D_h^{fr}} \quad (14)$$

$$c_p^{fr} \frac{dT^{fr}}{dz} = f^{fr} \frac{v^{fr}}{|v^{fr}|} \frac{M^{fr} (v^{fr})^2}{2D_h^{fr}} + \frac{W}{F^{fr}} (J_q - h^{fr} J) - \sum_i h_i^{fr} \frac{dx_i^{fr}}{dz} \quad (15)$$

3.2. Transport between the air streams

Transport between the air streams can be described by use of flux-force relations from nonequilibrium thermodynamics [35]:

$$\Delta\left(\frac{1}{T}\right) = r_q J_q^{ex} \quad (16)$$

$$-\Delta\left(\frac{\mu_w}{T}\right) + h_w^{ex} \Delta\left(\frac{1}{T}\right) = r_w J_w \quad (17)$$

where μ_w is the chemical potential of water, r_q and r_w are the heat and mass transport coefficients, and $J_q^{ex} = J_q - J_w h_w^{ex}$ is the measurable heat flux on the exhaust air side. We use the symbol Δ to indicate the difference in thermodynamic variables between the two sides. The left-hand sides of Eqs. 16-17 represent the driving forces for heat and mass transport. Coupling between fluxes has been neglected because they are most often small in comparison to the main transport contributions.

Two main phenomena contribute to the transport coefficients. The first contribution is due to the resistance to transport offered by the wall between the two streams. The second contribution is given by the resistance to transport of the convective boundary layers that form in the fluid on each side of the separating wall. The calculation of the transport coefficients is further discussed in Appendix A.

3.3. Second-law energy efficiency and loss of useful work

For a recovery ventilator, the second-law efficiency can be defined as [32]:

$$\eta_{II} = 1 - \frac{W_{lost}}{W_{ideal}} \quad (18)$$

where W_{ideal} is the maximum useful work that can be extracted from the exhaust air that enters the recovery ventilator, and W_{lost} is the useful work that is lost in the process. Two main phenomena contribute to the overall lost work:

$$W_{lost} = W_{irr} + W_{amb} \quad (19)$$

where W_{irr} is the lost work due to irreversibilities inside the system, and W_{amb} is the useful work that is lost by discharging the exhaust air in the outdoor ambient.

The work that is lost due to irriversibilities is directly related to the total entropy that is produced during the process, Σ_{irr} , by the Gouy–Stodola theorem [37]:

$$W_{irr} = T_0 \Sigma_{irr} \quad (20)$$

where T_0 is the temperature of the ambient. The total entropy production of the process is the integral of the local entropy production of a system cross section, σ , over the system length, L [35]:

$$\Sigma_{irr} = \int_0^L \sigma \, dz \quad (21)$$

The entropy production can be written as sum of the products of all thermodynamic forces in the system and their conjugated fluxes [35]. Thus, for the present case, the local entropy production is:

$$\begin{aligned} \sigma = & J_q^{ex} \Delta \left(\frac{1}{T} \right) + J_w \left(-\Delta \left(\frac{\mu_w}{T} \right) + h_w^{ex} \Delta \left(\frac{1}{T} \right) \right) \\ & + A^{ex} v^{ex} \left(-\frac{1}{T^{ex}} \frac{dp^{ex}}{dz} \right) + A^{fr} v^{fr} \left(-\frac{1}{T^{fr}} \frac{dp^{fr}}{dz} \right) \end{aligned} \quad (22)$$

where the first term on the right-hand side represents the product between the measurable heat flux and the thermal driving force, and the second is the product between the mass flux and the chemical driving force. The last two terms represent the entropy production due to friction, where the flux is the stream velocity and the viscous flow driving force is $\left(-\frac{1}{T} \frac{dp}{dz} \right)$.

The total entropy production can also be calculated from the entropy balance on the system, as presented in Appendix B. The alternative formulation given by Eq. B.1 does not require detailed knowledge of the thermodynamic variables across the system, but relies exclusively on inlet and outlet values of the variables. However, it does not localize where entropy is produced in the system and by what phenomena. This information can be used in designing, improving and optimizing recovery devices.

The ideal work that can be extracted from the exhaust air is equivalent to the exergy of the stream [31]:

$$\begin{aligned} W_{ideal} = & F_{in}^{ex} \left(h_{in}^{ex} - h_{in,0}^{ex} - T_0 \left(s_{in}^{ex} - s_{in,0}^{ex} \right) \right) \\ & + F_{in}^{ex} R T_0 \sum_i x_{i,in}^{ex} \ln \left(\frac{x_{i,in}^{ex}}{x_{i,0}} \right) \end{aligned} \quad (23)$$

where s_{in}^{ex} is the molar entropy of the inlet exhaust air, $h_{in,0}^{ex}$ and $s_{in,0}^{ex}$ are the enthalpy and entropy of the gas evaluated at the temperature and pressure of the ambient (i.e. T_0 and p_0), and $x_{i,0}$ is the reference composition of the ambient. The subscript *in* indicates the thermodynamic variable at the inlet of the considered air stream. The first term on the right-hand side of Eq. 23 represents the physical contribution to the ideal work, $W_{ideal,ph}$, while the second term represents the chemical contribution, $W_{ideal,ch}$ [31].

Since the fresh air stream enters the recovery ventilator at ambient conditions, no useful work can be extracted from it.

The work that is lost to the ambient corresponds to the exergy that is destroyed by discharging the exhaust air stream in the ambient:

$$\begin{aligned} W_{amb} &= F_{out}^{ex} \left(h_{out}^{ex} - h_{out,0}^{ex} - T_0 (s_{out}^{ex} - s_{out,0}^{ex}) \right) \\ &\quad + F_{out}^{ex} R T_0 \sum_i x_{i,out}^{ex} \ln \left(\frac{x_{i,out}^{ex}}{x_{i,0}} \right) \\ &= W_{amb,ph} + W_{amb,ch} \end{aligned} \quad (24)$$

where $h_{out,0}^{ex}$ and $s_{out,0}^{ex}$ are the enthalpy and the entropy of the gas evaluated at T_0 and p_0 . The subscript *out* indicates the thermodynamic variable at the outlet of the considered air stream. Here, $W_{amb,ph}$ and $W_{amb,ch}$ are the physical and the chemical contributions to the work lost to ambient.

We notice that since the inlet conditions of the exhaust air and those of the ambient are fixed, the denominator of Eq. 18 is the same for both the HRV and the MERV.

4. Case specification

4.1. Relevant data

The most relevant data used in the calculations are summarized in Table 1. We adopt a target indoor relative humidity, RH_{in}^{ex} , of 40 %, and indoor temperature of 294 K, which lie in the range of indoor humidities and temperatures recommended by the Norwegian building code [14]. We consider a range of outdoor temperatures, typical of both cold and warm climates.

The geometrical configuration of the two systems is the same, but they differ in structural and physical characteristics of the wall that separates the air streams. The geometrical parameters and the wall properties in Table 1 are used to calculate the transport coefficients in Table 2. Usually, the air channels contain spacers that improve the structural integrity channels and enhance heat and mass transfer. However, the presence of spacers makes the friction factor and, therefore, the pressure drops larger (Eq. 7 and Eq. 14). We use the relation for friction factor in ducts with spacers determined by the experimental work in Ref. [39].

In order to obtain a larger exchange area between the two streams, several air channels are alternately stacked on top of each other to obtain a convenient configuration of the system. Because of symmetry, the complex stacked system can be described by a single pair of exhaust/fresh air channels, where the height of the channel is half of the one of a single channel, $H = H_{duct}/2$, and the width is double that of a single channel multiplied by the number of channel pairs, $W = 2W_{duct}N$.

Table 1: Operating conditions and structural and physical parameters assumed in calculations.

Symbol	Value	Unit	Ref.
p_0	10^5	Pa	
Indoor environment			
T^{indoor}	294	K	[14]
RH^{indoor}	40	%	[14]
v_{in}^{ex}	0.6	m s^{-1}	
Outdoor ambient			
T_0	263-303	K	
RH_0	10-90	%	
Geometrical parameters			
L	0.185	m	[24]
W_{duct}	0.185	m	[24]
$H_{duct}^{ex}, H_{duct}^{fr}$	$4.0 \cdot 10^{-3}$	m	[24]
N	57	-	
HRV			
δ	$5.0 \cdot 10^{-4}$	m	
λ^{wall}	$2.0 \cdot 10^2$	$\text{W m}^{-1} \text{K}^{-1}$	
P_w	0	$\text{kmol Pa}^{-1} \text{s}^{-1} \text{m}^{-1}$	
MERV			
δ	$102 \cdot 10^{-6}$	m	[24]
λ^{wall}	0.13	$\text{W m}^{-1} \text{K}^{-1}$	[24]
P_w	$1.0 \cdot 10^{-13}$	$\text{kmol Pa}^{-1} \text{s}^{-1} \text{m}^{-1}$	[38]

4.2. Boundary conditions

In order to solve the set of eight ODEs, we need to impose eight boundary conditions:

$$T_{in}^{ex} = T^{indoor} \quad (25)$$

$$F_{in}^{ex} = A^{ex} \frac{v_{in}^{ex} p_0}{RT^{indoor}} \quad (26)$$

$$F_{w,in}^{ex} = F_{in}^{ex} x_w^{indoor} \quad (27)$$

$$p_{out}^{ex} = p_0 \quad (28)$$

$$T_{in}^{fr} = T_0 \quad (29)$$

$$F_{a,in}^{fr} = F_{a,in}^{ex} \quad (30)$$

$$F_{w,in}^{fr} = F_{a,in}^{fr} \frac{x_{w,0}}{1 - x_{w,0}} \quad (31)$$

$$p_{out}^{fr} = p_0 \quad (32)$$

The boundary condition values are calculated from the data reported in Table 1. In addition, we consider that the dry air stream extracted from the indoor environment needs to be the same as the dry air stream supplied from the outdoor ambient.

Table 2: Calculated transport coefficients for the HRV and for the MERV, at $z = L/2$. Calculations are carried out at $T_0 = 263$ K and $RH_0 = 60$ %.

	HRV	MERV	Unit
$r_q^{h,conv}$	$1.4 \cdot 10^{-7}$	$1.4 \cdot 10^{-7}$	$\text{m}^2 \text{ s J}^{-1} \text{ K}^{-1}$
r_q^{wall}	$2.7 \cdot 10^{-11}$	$8.8 \cdot 10^{-9}$	$\text{m}^2 \text{ s J}^{-1} \text{ K}^{-1}$
$r_q^{c,conv}$	$1.5 \cdot 10^{-7}$	$1.5 \cdot 10^{-7}$	$\text{m}^2 \text{ s J}^{-1} \text{ K}^{-1}$
$r_w^{h,conv}$	-	$2.6 \cdot 10^6$	$\text{m}^2 \text{ s J K}^{-1} \text{ kmol}^{-2}$
r_w^{wall}	-	$4.5 \cdot 10^9$	$\text{m}^2 \text{ s J K}^{-1} \text{ kmol}^{-2}$
$r_w^{c,conv}$	-	$2.6 \cdot 10^6$	$\text{m}^2 \text{ s J K}^{-1} \text{ kmol}^{-2}$

5. Solution procedure

With the given assumptions, the system is properly described by a set of eight ordinary differential equations (Eqs. 4-5, Eq. 11, Eq. 7, and Eqs. 12-14). Since the boundary conditions are specified at both ends of the system (Section 4.2), the problem is a two-point boundary value problem. The problem is solved by use of the MATLAB `bvp4c`-solver, which is a collocation solver that implements the three-stage Lobatto IIIa formula and bases the mesh selection and error control on the residual of the solution [40].

6. Model validation

Heat and moisture exchange effectiveness, ϵ_s and ϵ_w , are two of the parameters that are most commonly used in the literature to characterize recovery performance. Most published research uses heat and moisture effectiveness as a criterion to validate the accuracy of simulations as well as of experiments [30]. Widely used empirical relations exist to calculate the heat and moisture effectiveness based on the design parameters of the HRV/MERV (i.e. the number of transfer unit for transport of heat and moisture, NTU_s and NTU_w) [41, 42]. In order to verify the accuracy of the model, the computed heat and moisture effectiveness were compared to those predicted by the ϵ - NTU relations that was developed in References [41] and [42]. The results agree within 1.6 % (with the exception of a narrow range of outdoor conditions where ϵ_s diverges), indicating that the model gives a good description of real recovery ventilator. Moreover, the results of the sensitivity analysis in Appendix C show that uncertainty in the input parameters does not significantly affect the results and that no unexpected relationships between inputs and outputs are revealed.

7. Results

7.1. Transport between streams

Two main phenomena contribute to the overall heat and mass transport coefficients. One contribution is due to the heat transport resistance of the wall material, while a second contribution depends on transport across the convective boundary layers adjacent

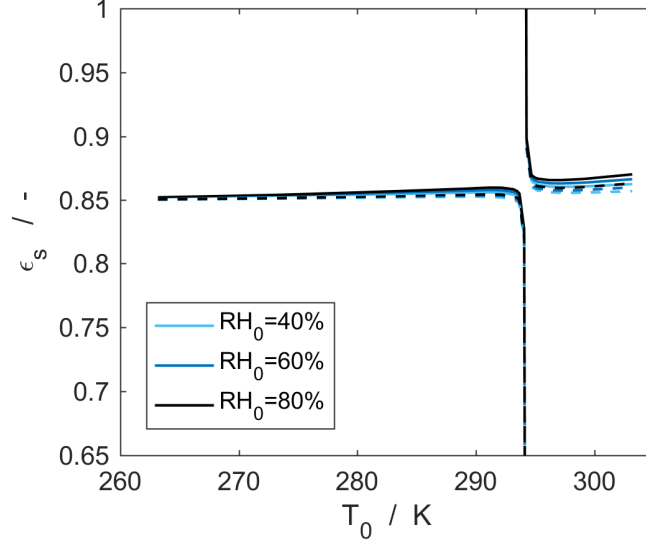


Figure 2: Sensible heat exchange effectiveness, ϵ_s , for the HRV (solid lines) and for the MERV (dashed lines), for $RH_0 = 40\%$ (light blue lines), $RH_0 = 60\%$ (blue lines), and $RH_0 = 80\%$ (black lines). At $T_0 = T_{indoor}$, ϵ_s is not defined.

to the separating wall. Table 2 presents the different contributions to the total heat and mass transport coefficients in the HRV and MERV as calculated according to the equations presented in Appendix A. The convective layers are responsible for most of the heat transport resistance. In the HRV, the convective resistances to heat transport are four orders larger than that due to conduction across the separating wall. This justifies the common practice of neglecting the wall conductive resistance [30] for this case. Membrane materials for MERV typically have a lower thermal conductivity than the metallic materials in HRV (three orders of magnitude lower, in the present case). The resistance to conductive heat transport is small in comparison to the convective resistance even in the case of the MERV, contributing only 3.5 % to the total resistance.

In contrast to the case of heat transport, the main resistance to mass transport is caused by diffusion through the membrane material. In the present case, the convective resistance is only 0.1 % of the total resistance to mass transport. Convective transport may however play a more important role under different operating conditions as other studies have reported convective contributions to water mass transport as high as 30 % for different flow regimes [28].

7.2. Heat and moisture effectiveness and second-law energy efficiency

Figure 2 shows the sensible heat exchange effectiveness of the HRV (solid lines) and of the MERV (dashed lines) calculated according to Eq. 1. The sensible effectiveness is very similar for the HRV and the MERV for all considered outdoor temperatures and relative humidities. The slightly higher ϵ_s for the HRV is due to the lower

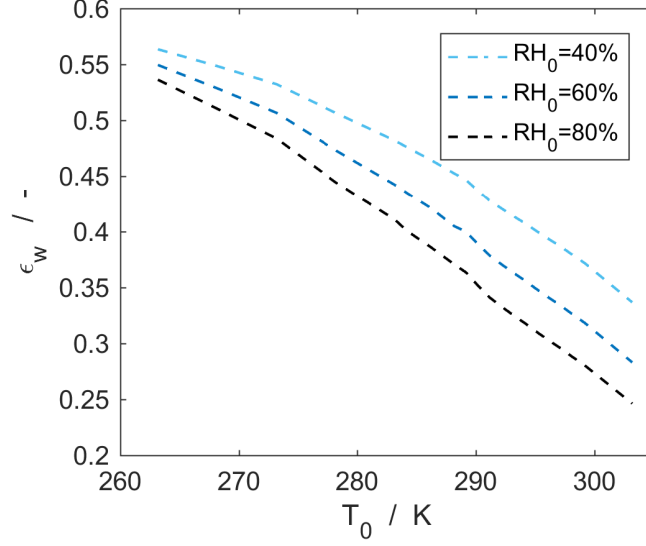


Figure 3: Moisture exchange effectiveness, ϵ_w for the MERV (dashed line) as functions of the outdoor temperature, for $RH_0 = 40\%$ (light blue line), $RH_0 = 60\%$ (blue line), and $RH_0 = 80\%$ (black line). Since HRV does not exchange any water, ϵ_w is everywhere zero for the HRV. At $x_{w,0} = x_w^{indoor}$, ϵ_w is not defined.

resistance to heat transport offered by the metal wall that separates the streams. The sensible effectiveness does not have a strong dependence on the outdoor conditions, and increases only slightly for higher outdoor temperatures. Since the denominator in Eq. 1 is zero when the outdoor and indoor temperatures are equal (at $T_0 = T^{indoor}$ thin dotted line), ϵ_s cannot be defined for this case. Because of the friction term in the energy balance equation (first term on the right-hand side of Eq. 11), a small increase of the exhausted stream temperature occurs even when indoor and outdoor temperatures are equal. This phenomenon makes ϵ_s diverge for outdoor temperatures close to the indoor temperature.

Figure 3 represents the moisture transfer effectiveness, ϵ_w , for the MERV (dashed lines) as a function of the outdoor temperature, for $RH_0 = 40\%$ (light blue line), $RH_0 = 60\%$ (blue line), and $RH_0 = 80\%$ (black line). In the HRV, the air streams do not exchange any moisture, and this parameter is always zero. For the MERV, ϵ_w decreases with decreasing outdoor temperature. Similar behaviour has been observed by others (e.g. the experimental work in Reference [28]). When the water mole fractions of the indoor and outdoor air are equal ϵ_w is not defined.

Figure 4 illustrates the second-law efficiency of the HRV (solid lines) and the MERV (dashed lines). The behavior of η_{II} as a function of the ambient temperature is very complex, however it is similar for different outdoor relative humidities. In cold climates, for $RH_0 = 60\%$ (blue line), and $RH_0 = 80\%$ (black line), η_{II} of the HRV increases as the outdoor temperature increases, until it reaches the value for which indoor and outdoor water molar fraction are the same, $x_w^{indoor} = x_{w,0}$. For a further increase

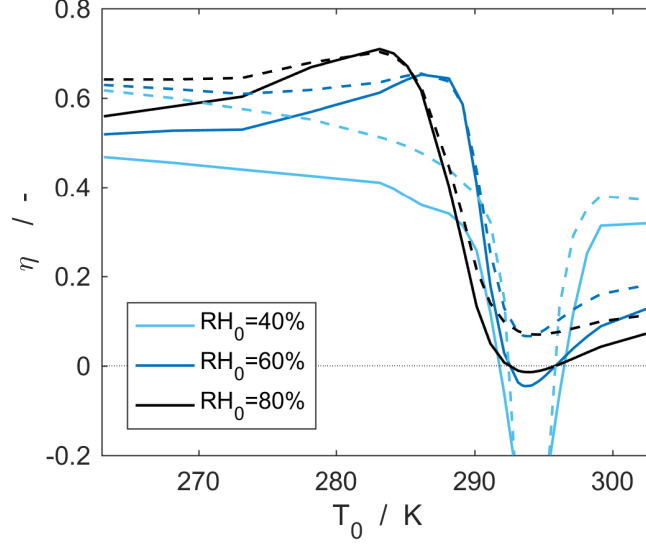


Figure 4: Second-law energy efficiency, η_{II} , for the HRV (solid lines) and for the MERV (light blue lines) as functions of the outdoor temperature, for $RH_0 = 40\%$ (red lines), $RH_0 = 60\%$ (blue lines), and $RH_0 = 80\%$ (black lines).

of T_0 , η_{II} drops. When $T^{indoor} = T_0$, the second-law efficiency of the HRV is negative, since useful work is lost, due to pressure drops, without generating any useful output. For T_0 higher than the indoor temperature, η_{II} increases with increasing ambient temperature. When $x_w^{indoor} = x_{w,0}$, the air streams cannot exchange moisture in any of the configurations, and the efficiencies of the HRV and MERV are approximately the same. For $RH_0 = 40\%$ (red lines), x_w^{indoor} and $x_{w,0}$ are the same when $T^{indoor} = T_0$. Under such conditions, no useful work can be recovered from the exhausted stream, and the second-law efficiency is not defined.

For the MERV, η_{II} is roughly constant both in cold and warm climates, and it drops from one value to the other in the temperature interval between the conditions for which $x_w^{indoor} = x_{w,0}$ and $T^{indoor} = T_0$. The comparison between the two systems shows that the second-law efficiency of the MERV is never smaller than that of the HRV. In cold climates, the difference between the two efficiencies increases with decreasing temperature. For $RH_0 = 60\%$ (blue dashed line) and $RH_0 = 80\%$ (black dashed line), the η_{II} of the MERV is never negative. However, for temperatures and water fraction of the outside air equal to those of the indoor space, the MERV second-law efficiency is negative (light blue dashed line), indicating that no net benefit is obtained from the recovery ventilator. Instead, it is detrimental to the performance of the ventilation system as electric energy is expended to compensate for pressure drop. Under such conditions it would be better to let the air streams bypass the recovery unit.

Figure 5 shows how the second-law efficiency of the HRV (solid line) and of the MERV (dashed line) varies as a function of the exhaust air volume flow rate. The air

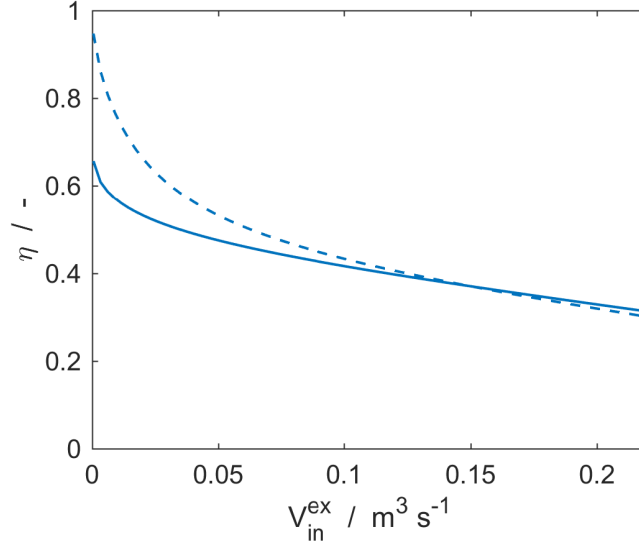


Figure 5: Second-law energy efficiency, η_{II} , for the HRV (solid line) and for the MERV (dashed line) as functions of the volume flow rate. Calculations are carried out at $T_0 = 263$ K and $RH_0 = 60$ %.

flow rate is varied within a range that allows for the air velocity to stay under 5 m s^{-1} , in order to avoid unnecessary noise generation. The second-law efficiency is largest when the flow rate approaches zero, and it decreases for increasing flow rates. There is thus a trade-off between the air that can be treated by a ventilator of a given size and the resulting second-law efficiency. A larger HRV/MERV will retain a high efficiency for larger flow rates, but would require larger investment costs. In practice, the air volume flow rate is determined by the size of the building and by the rate at which the indoor air needs to be replaced. The latter is often dictated by local regulations, e.g. [14]. With the flow rate given, one may choose an acceptable η_{II} and increase the size of HRV/MERV, or change other design parameters, until the desired efficiency is achieved. This is one example of a way in which the second-law efficiency may guide the design and sizing of such devices.

Figure 5 shows that for high flow rates the second-law efficiency of the HRV is higher than that of the MERV. This is due to the fact that the mass transport resistance is large in comparison to that of heat transport. Therefore, the transport of heat is more facile than the mass transport. Accordingly, for high air velocities, the water recovery is very low, and heat recovery represents the dominant contribution to the second-law efficiency. The resistance to convective heat transport decreases with increasing flow rate and, hence the wall heat transport resistance becomes relatively more important. Since the wall thermal resistance of the MERV is two orders of magnitude larger than that of the HRV, the MERV heat recovery and second-law efficiency are smaller than those of the HRV.

Figures 6 and 7 show the second-law efficiency as function of both outdoor tem-

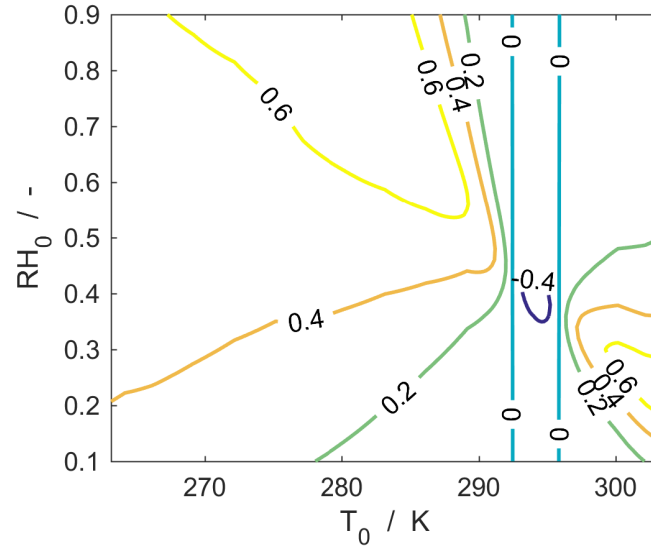


Figure 6: Second-law energy efficiency, η_{II} , for the HRV as function of the outdoor ambient temperature and of the outdoor relative humidity.

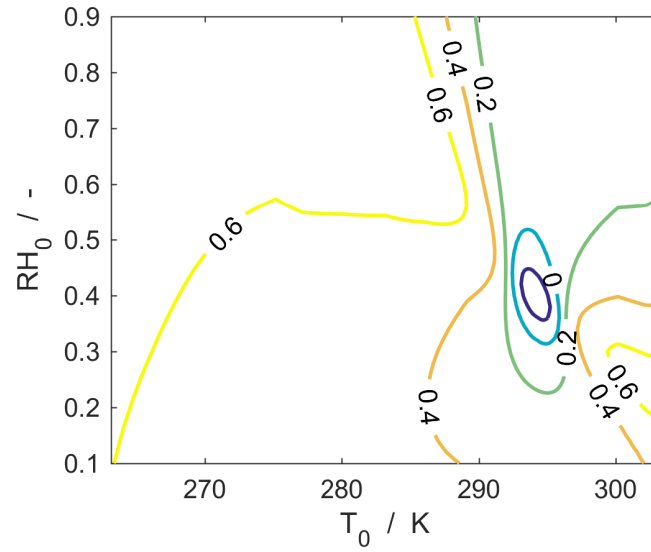


Figure 7: Second-law energy efficiency, η_{II} , for the MERV as function of the outdoor ambient temperature and of the outdoor relative humidity.

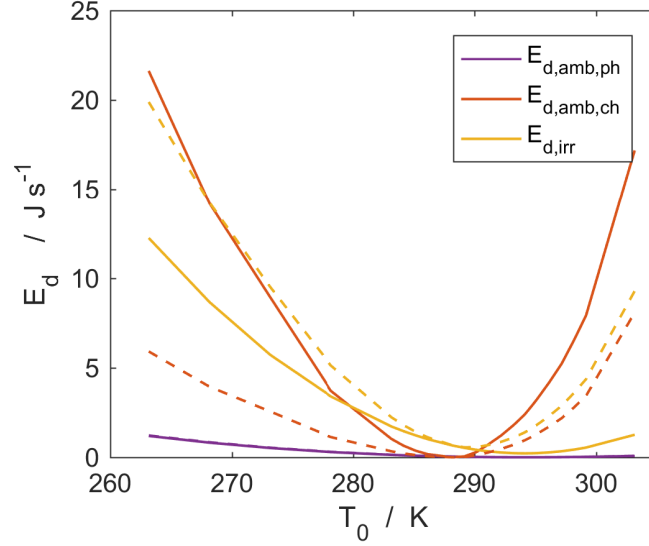


Figure 8: Physical useful work lost to the ambient, $W_{amb,ph}$ (purple lines), chemical useful work lost to the ambient, $W_{amb,ch}$ (orange lines), and useful work lost to irreversibilities, W_{irr} (yellow lines), for the HRV (solid lines) and for the MERV (dashed lines) as functions of the outdoor temperature. The solid and dashed purple lines ($W_{amb,ph}$) coincide at the scale of the representation. Calculations are carried out at $RH_0 = 60\%$.

perature and relative humidity. These figures are useful e.g. to identify the range of outdoor conditions for which the recovery ventilator is responsible for increasing the energy need of the building (area enclosed by the light blue lines where η_{II} is zero). Under such conditions, it is more beneficial to bypass the HRV/MERV. The comparison between the two pictures shows that the range of unfavorable outdoor conditions is much smaller for the MERV than for the HRV. Moreover, the MERV retains a second-law efficiency larger than 60 % in a larger portion of the outdoor condition space.

In the present case, pressure losses are low, and thus the operational range for which η_{II} is negative is small. However, under different operating conditions and configurations (e.g. higher air velocities or larger friction coefficients inside the ducts), such losses could have larger influence on the overall performance, and enlarge the range of operating conditions for which the use of a HRV/MERV is not beneficial.

The comparison between ϵ_s , ϵ_w and the second-law efficiency shows that these three parameters have very different behaviors, and that the combination of ϵ_s , ϵ_w into a single performance indicator is not straightforward. Performance analysis based on ϵ_s and ϵ_w can therefore create difficulties in the comparison of different solutions, especially when alternatives where only heat is recovered need to be compared with solutions where both heat and moisture are recovered.

Figure 8 shows the contributions to the loss of useful work due to physical (purple-black lines) and chemical (orange-blue lines) work lost to the ambient, and due to the work lost to irreversibilities in the system (yellow-red lines), for the HRV (solid lines) and for the MERV (dashed lines) for $RH_0 = 60\%$. Similar results are obtained for the

other considered outdoor relative humidity (not reported here).

The physical lost work, $W_{amb,ph}$, is approximately the same for the two systems (solid and dashed purpleblack lines coincides at the plot accuracy), since the outlet temperature of the exhaust air is about the same in the HRV and MERV. Moreover, the loss of physical work is quite small in comparison to the other work losses, especially at very low and at very high outdoor temperatures.

On the other hand, the chemical lost work is much larger in the HRV than in the MERV, since none of the moisture in the exhaust air is recovered. Thus, all the ideal chemical potential work of the inlet exhaust air is lost.

The loss of work potential due to irreversibilities in the MERV is always larger than in the case of the HRV. Indeed, W_{irr} strongly depends on the heat and mass transfer and on the pressure drops in the system (see Eq. 22). Since the contributions due to heat transfer and pressure drops are approximately the same in the two systems, the difference between W_{irr} is mainly due to the additional contribution of moisture transport in the MERV. The work lost due to irreversibilities goes through a minimum. For the HRV, minimum W_{irr} is obtained for $T^{indoor} = T_0$. Under these conditions, no heat is exchanged between the air streams, and the only contribution to W_{irr} is due to the pressure drops. In the MERV, the minimum in W_{irr} is located between the outdoor conditions for which the sensible heat transfer is zero ($T^{indoor} = T_0$), and the condition for which the moisture transfer is zero ($x_w^{indoor} = x_{w,0}$).

The overall work that is lost in the system gives an indication of the energy that one needs to supply to the indoor ambient to maintain temperature and humidity levels that are compatible with comfortable indoor conditions. In order to maintain comfort, the ventilation system is normally coupled with auxiliary systems that compensate for the work lost during ventilation. In particular, auxiliary systems add or remove sensible heat from the indoor air (e.g. radiators or air conditioners), others control the moisture level (e.g. dehumidifiers or humidifiers), while fans compensate for the pressure drops in the ventilation system. The knowledge on the different contributions to the lost work allows us to locate and compare the ideal amount of energy needed by the different auxiliary systems to maintain the desired temperature and humidity levels. Since different auxiliary systems might be supplied by different energy sources, this approach makes it easier to include considerations on the primary energy use of buildings.

Figure 8 shows that, for the HRV, most of the energy that needs to be supplied to the system is used for moisture control, both in cold and warm climates. With the use of the MERV in cold climates, the energy used for such purpose is reduced to a level similar to that needed for temperature control. This is not the case for warm climates. For ambient temperatures close to that of the indoor temperature, the use of the HRV is not beneficial, since it increases the fan power, without bringing any recovery of heat or moisture. On the other hand, due to moisture exchange, the use of the MERV remains beneficial for ambient temperatures close to the indoor one, when the indoor and outdoor water content is different.

8. Conclusions

We have used second-law analysis to characterize the performance of heat and energy recovery ventilators. We considered and compared the performances of a heat

recovery ventilator (HRV) and those of a structurally similar membrane energy recovery ventilator (MERV). The use of second-law analysis made it possible to quantify, assess and compare the performances of HRV/MERV in terms of a single parameter, the second-law efficiency. This parameter describes the loss of work potential and may account for all different sources of work loss and for differences in energy quality.

Traditional effectiveness parameters defined by Eqs. 1-3 are most commonly used in literature to characterize recovery ventilators performance. In the considered cases, the sensible heat exchange effectiveness was not significantly different for the HRV and the MERV, and it showed only a weak dependence on the outdoor temperature. The MERV moisture exchange effectiveness decreased as the outdoor temperature increased. This is always zero in the HRV. While useful by themselves, these effectiveness parameters are difficult to compare and relate to each other. Since there is no obvious optimal trade-off between them, it is challenging to combine them in a way that allows for a sensible comparison of different technical solutions such as the HRV and MERV.

We showed that the second-law efficiency can be used to identify the range of operating conditions for which the recovery ventilator is responsible for increasing the energy need of the building, and for which it is more beneficial to bypass the HRV/MERV. When the second-law efficiency is negative, the recovered heat and moisture are not enough to compensate for the fan power necessary drive the air flow in the recovery unit. Such phenomenon cannot trivially be predicted by the traditional performance parameters.

Because of the additional moisture recovery, the MERV was beneficial for a broader range of ambient conditions than the HRV. The second-law efficiency showed that a big potential exists to improve recovery systems, especially in warm climates, where η_{II} can be very low.

The second-law analysis additionally enabled the localization and comparison of the various components of the loss of useful work in the systems. This means that it is a tool that can be used not just to assess the efficiency of the process, but also one that can be used to optimize the design of the devices used in the process.

Acknowledgments

The Norwegian University for Science and Technology and the VISTA program, a basic research program in collaboration with The Norwegian Academy of Science and Letters and Statoil, are acknowledged for financial support.

Appendix A. Transport coefficients

The transport coefficients have two main contributions. A first contribution is due to the resistance to transport offered by the wall separating the two streams, r_i^{wall} . A second contribution is given by the resistance offered by the convective boundary layers that are present at the two sides of the separating wall, $r_i^{h,conv}$ and $r_i^{c,conv}$. Similarly to resistances in series, the overall transport coefficients can be written as:

$$r_i = r_i^{h,conv} + r_i^{wall} + r_i^{c,conv} \quad (A.1)$$

Appendix A.1. Heat transport coefficients

The wall heat transport coefficient can be derived from experimental data on the thermal conductivity of the wall material. Thermal conductivity experiments are typically carried out at zero mass flux. According to Fourier's law, the measurable heat flux is:

$$J'_q = -\lambda^{wall} \frac{\Delta T}{\delta} \quad (\text{A.2})$$

where λ^{wall} is the thermal conductivity of the wall material, and δ is the wall thickness. By comparing Eq. A.2 and Eq. 16, we can relate the wall heat transport coefficient to the experimental thermal conductivity of the wall material:

$$r_q^{wall} = \frac{\delta}{\lambda^{wall} T^2} \quad (\text{A.3})$$

The heat transport resistance due to the convective boundary layer can be calculated from the convective heat transfer coefficient, h^{conv} , which is defined as:

$$J'_q = -h^{conv} \Delta T \quad (\text{A.4})$$

where ΔT is the difference in temperature between the membrane surface and the gas bulk. The coefficient depends on the characteristics of the flow, and it is related to the Nusselt number by the following relation:

$$h^{conv} = \text{Nu} \frac{\lambda}{D_h} \quad (\text{A.5})$$

where λ is the thermal conductivity of the fluid. Empiric relations exist that relate the Nusselt number to the characteristics of the flow. In order to maintain the channel geometry and to enhance heat and mass transfer, spacers are usually present in the air channels. In this work, we use the correlations for Nusselt number that have been established for flow in ducts with spacers [39]:

$$\text{Nu} = j \text{RePr}^{1/3} \quad (\text{A.6})$$

where j is the Colburn heat transfer factor, Re is the Reynolds number, and Pr is the Prandtl number. The Colburn heat transport factor is determined experimentally as a function of the Reynolds number [39]:

$$j = \frac{C_0}{\text{Re}^m} \quad (\text{A.7})$$

where C_0 and m are two fitted parameters.

By comparing Eq. A.5 with Eq. 16, we can relate the convective heat transport resistance to the convective heat transport coefficient:

$$r_q^{conv} = \frac{1}{h^{conv} T^2} \quad (\text{A.8})$$

Appendix A.2. Mass transport coefficients

Mass transport through semi-permeable membranes is usually characterized by permeability parameters. The permeability of a material to a component is determined experimentally at isothermal conditions (i.e. $\Delta T=0$). In the present case, the membrane permeability to water, P_w , is defined as:

$$J_w = -P_w \frac{\Delta p_w}{\delta} \quad (\text{A.9})$$

where Δp_w is the the water partial pressure difference between the two sides of the membrane. By comparing Eq. A.9 with Eq. 17, we can relate the membrane mass transport resistance to the permeability:

$$r_w^{wall} = \frac{\delta}{TP_w} \frac{\Delta \mu_w}{\Delta p_w} \quad (\text{A.10})$$

The convective resistance to water transport can be calculated from the convective mass transport coefficient, k^{conv} , which is defined as [36]:

$$J_w = -k^{conv} \Delta c_w \quad (\text{A.11})$$

where c_w is the water molar concentration. For air-water vapor mixtures, the convective mass transport coefficient can be expressed with good accuracy by the Lewis relation [36]:

$$k^{conv} = \frac{h^{conv}}{c_p c} \quad (\text{A.12})$$

where c and c_p are the molar concentration and the molar heat capacity of humid air. The comparison of Eq. A.11 with Eq. 17 gives:

$$r_w^{conv} = \frac{1}{Tk^{conv}} \frac{\Delta \mu_w}{\Delta c_w} \quad (\text{A.13})$$

Appendix B. Total entropy production from the entropy balance on the system

In a steady state, the total entropy production of a process can also be calculated from the entropy balance on the system [35]:

$$\begin{aligned} \Sigma_{irr} &= (S_{out}^{ex} + S_{out}^{fr}) - (S_{in}^{ex} + S_{in}^{fr}) \\ &= (F_{out}^{ex} S_{out}^{ex} + F_{out}^{fr} S_{out}^{fr}) - (F_{in}^{ex} S_{in}^{ex} + F_{in}^{fr} S_{in}^{fr}) \end{aligned} \quad (\text{B.1})$$

where S is entropy flow. With this formulation, the total entropy production can be calculated from the knowledge of flow rates, temperature, composition, and pressure at the inlet and outlet of the system only. Therefore, we do not need any additional information than the one needed to calculate the effectiveness parameters according to Eqs. 1-3.

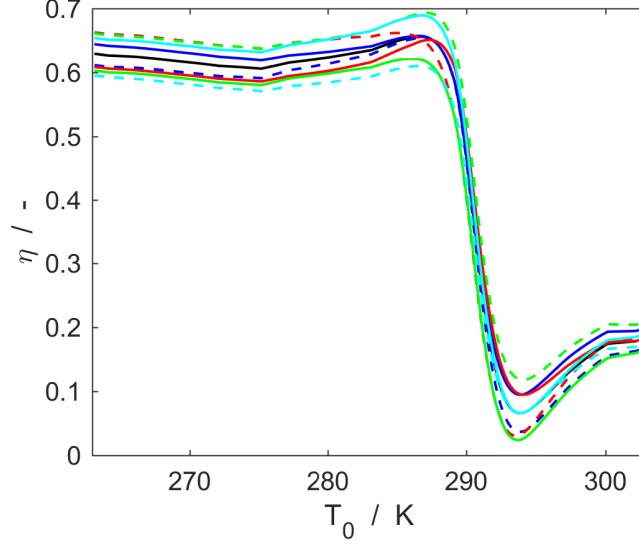


Figure C.1: Second-law efficiency, η_{II} , of the MERV as a function of the outdoor temperature, for variation of the considered input parameter of 20 % (solid lines) and -20 % (dashed lines). The considered input parameters are duct height (red lines), membrane permeability (blue lines), inlet air velocity (green lines), and convective heat transport coefficient (light blue lines). The black line represent the results for unvaried input parameters. Calculations are carried out at $T_0 = 263$ K and $RH_0 = 60$ %.

Appendix C. Sensitivity analysis

The sensitivity analysis is carried out with a dual purpose. First, the analysis allows us to test the sensitivity of the results to uncertainties in the input parameters. Second, it enables us to obtain a deeper understanding of the relationships between input parameters and results and to possibly reveal any errors in the model, if unexpected behaviors should appear. The input parameters considered in the analysis are duct height, $H_{duct}^{ex} = H_{duct}^{ex}$, membrane permeability, P_w , and inlet velocity of the exhausted air, v_{in}^{ex} , and convective heat transport coefficient, h_{conv} , which are varied from -20 % to 20 % of their original value reported in Table 1 or calculated according to Eq. A.5.

Figure C.1 reports the results of the sensitivity analysis for the second-law efficiency. The variation of the input parameters has only a modest impact on η_{II} . The maximum variation of η_{II} at 263 K is -5.2 % (obtained for -20 % variation of h_{conv}), while it is -9.3 % at 303 K (obtained for 20 % variation of the inlet air velocity).

References

- [1] D. Chwieduk, Towards sustainable-energy buildings, *Applied Energy* 76 (1) (2003) 211–217.

- [2] S. B. Sadineni, S. Madala, R. F. Boehm, Passive building energy savings: A review of building envelope components, *Renewable and Sustainable Energy Reviews* 15 (8) (2011) 3617–3631.
- [3] P. J. Walsh, C. S. Dudley, E. D. Copenhaver, *Indoor air quality*, CRC Press, 1983.
- [4] A. P. Jones, Indoor air quality and health, *Atmospheric Environment* 33 (28) (1999) 4535–4564.
- [5] K. Sakai, D. Norbäck, Y. Mi, E. Shibata, M. Kamijima, T. Yamada, Y. Takeuchi, A comparison of indoor air pollutants in Japan and Sweden: formaldehyde, nitrogen dioxide, and chlorinated volatile organic compounds, *Environmental Research* 94 (1) (2004) 75–85.
- [6] HVAC systems and equipment, *ASHRAE Handbook* (1996).
- [7] S. C. Sugarman, *HVAC fundamentals*, CRC Press, 2005.
- [8] P. O. Fanger, *Thermal comfort. Analysis and applications in environmental engineering*, Danish Technical Press, Copenhagen, Denmark, 1970.
- [9] M. Fehrm, W. Reiners, M. Ungemach, Exhaust air heat recovery in buildings, *International Journal of Refrigeration* 25 (4) (2002) 439–449.
- [10] A. M. Omer, Energy, environment and sustainable development, *Renewable and Sustainable Energy Reviews* 12 (9) (2008) 2265–2300.
- [11] L. Pérez-Lombard, J. Ortiz, C. Pout, A review on buildings energy consumption information, *Energy and Buildings* 40 (3) (2008) 394–398.
- [12] K. McCormick, L. Neij, *Experience of Policy Instruments for Energy Efficiency in Buildings in the Nordic Countries*, Lund University, 2009.
- [13] 62.2, Ventilation and Acceptable Indoor Air Quality in Low-rise Residential Buildings, *ASHRAE Standard* (2013).
- [14] Byggteknisk forskrift (TEK 10), Direktoratet for Byggkvalitet (2016).
- [15] W. A. Shurcliff, Air-to-air heat-exchangers for houses, *Annual Review of Energy* 13 (1) (1988) 1–22.
- [16] A. Mardiana-Idayu, S. Riffat, Review on heat recovery technologies for building applications, *Renewable and Sustainable Energy Reviews* 16 (2) (2012) 1241–1255.
- [17] S. Kakac, H. Liu, A. Pramuanjaroenkij, *Heat exchangers: selection, rating, and thermal design*, CRC Press, 2012.
- [18] L. Zhang, Y. Jiang, Heat and mass transfer in a membrane-based energy recovery ventilator, *Journal of Membrane Science* 163 (1) (1999) 29–38.

- [19] G. Vasilyev, I. A. Tabunshchikov, M. Brodach, V. Leskov, N. Mitrofanova, N. Timofeev, V. Gornov, G. Esaulov, Modeling moisture condensation in humid air flow in the course of cooling and heat recovery, *Energy and Buildings* 112 (2016) 93–100.
- [20] A. Dodoo, L. Gustavsson, R. Sathre, Primary energy implications of ventilation heat recovery in residential buildings, *Energy and Buildings* 43 (7) (2011) 1566–1572.
- [21] Y. Zhang, Y. Jiang, L. Z. Zhang, Y. Deng, Z. Jin, Analysis of thermal performance and energy savings of membrane based heat recovery ventilator, *Energy* 25 (6) (2000) 515–527.
- [22] L. Zhang, J. Niu, Performance comparisons of desiccant wheels for air dehumidification and enthalpy recovery, *Applied Thermal Engineering* 22 (12) (2002) 1347–1367.
- [23] M. A. Mandegari, H. Pahlavanzadeh, Introduction of a new definition for effectiveness of desiccant wheels, *Energy* 34 (6) (2009) 797–803.
- [24] L.-Z. Zhang, Heat and mass transfer in a quasi-counter flow membrane-based total heat exchanger, *International Journal of Heat and Mass Transfer* 53 (23) (2010) 5478–5486.
- [25] J. Liu, W. Li, J. Liu, B. Wang, Efficiency of energy recovery ventilator with various weathers and its energy saving performance in a residential apartment, *Energy and Buildings* 42 (1) (2010) 43–49.
- [26] J. Min, M. Su, Performance analysis of a membrane-based energy recovery ventilator: Effects of membrane spacing and thickness on the ventilator performance, *Applied Thermal Engineering* 30 (8) (2010) 991–997.
- [27] M. Nasif, R. Al-Waked, G. Morrison, M. Behnia, Membrane heat exchanger in hvac energy recovery systems, systems energy analysis, *Energy and Buildings* 42 (10) (2010) 1833–1840.
- [28] J. Min, M. Su, Performance analysis of a membrane-based energy recovery ventilator: Effects of outdoor air state, *Applied Thermal Engineering* 31 (17) (2011) 4036–4043.
- [29] S. Dugaria, L. Moro, D. Del Col, Modelling heat and mass transfer in a membrane-based air-to-air enthalpy exchanger, in: *Journal of Physics: Conference Series*, Vol. 655, IOP Publishing, 2015, p. 012035.
- [30] P. Liu, M. J. Alonso, H. M. Mathisen, C. Simonson, Energy transfer and energy saving potentials of air-to-air membrane energy exchanger for ventilation in cold climates, *Energy and Buildings* 135 (2017) 95–108.
- [31] T. J. Kotas, *The exergy method of thermal plant analysis*, Elsevier, London, 2013.

- [32] S. Kjelstrup, D. Bedeaux, E. Johannessen, J. Gross, Non-equilibrium thermodynamics for engineers, World Scientific Publishing, Singapore, 2010.
- [33] Exergy Analysis for Sustainable Buildings, ASHRAE Technical Committee 7.4. URL <https://tc0704.ashraetcs.org/>
- [34] K.-C. Noh, J. Hwang, The effect of ventilation rate and filter performance on indoor particle concentration and fan power consumption in a residential housing unit, Indoor and Built Environment.
- [35] S. Kjelstrup, D. Bedeaux, Non-equilibrium thermodynamics of heterogeneous systems, Vol. 16, World Scientific, Singapore, 2008.
- [36] Y. A. Cengel, A. J. Ghajar, H. Ma, Heat and Mass Transfer: Fundamentals & Applications, McGraw-Hill, New York, 2011.
- [37] G. Gouy, Sur l'énergie utilisable, Journal de Physique 8 (1889) 501–518.
- [38] R. N. Huizing, F. K. Ko, Selective water vapour transport membranes comprising a nanofibrous layer and methods for making the same, US Patent 8,936,668 (Jan. 20 2015).
- [39] J. Woods, E. Kozubal, Heat transfer and pressure drop in spacer-filled channels for membrane energy recovery ventilators, Applied Thermal Engineering 50 (1) (2013) 868–876.
- [40] L. F. Shampine, J. Kierzenka, M. W. Reichelt, Solving boundary value problems for ordinary differential equations in MATLAB with bvp4c, Tutorial Notes (2000) 437–448.
- [41] W. M. Kays, A. L. London, Compact heat exchangers, McGraw-Hill, New York, NY, 1984.
- [42] L. Zhang, J. Niu, Effectiveness correlations for heat and moisture transfer processes in an enthalpy exchanger with membrane cores, Transactions-American Society of Mechanical Engineers Journal of Heat Transfer 124 (5) (2002) 922–929.